

# SET levels contribute to cohesion fatigue

Lu Yang<sup>a</sup>, Qian Zhang<sup>a</sup>, Tianhua Niu<sup>a</sup>, and Hong Liu<sup>a,b,c,\*</sup>

<sup>a</sup>Department of Biochemistry and Molecular Biology; <sup>b</sup>Tulane Cancer Center, and <sup>c</sup>Tulane Aging Center, Tulane University School of Medicine, New Orleans, LA 70112

**ABSTRACT** Chromosome instability (CIN) is a major hallmark of cancer cells and believed to drive tumor progression. Several cellular defects including weak centromeric cohesion are proposed to promote CIN, but the molecular mechanisms underlying these defects are poorly understood. In a screening for SET protein levels in various cancer cell lines, we found that most of the cancer cells exhibit higher SET protein levels than nontransformed cells, including RPE-1. Cancer cells with elevated SET often show weak centromeric cohesion, revealed by MG132-induced cohesion fatigue. Partial SET knockdown largely strengthens centromeric cohesion in cancer cells without increasing overall phosphatase 2A (PP2A) activity. Pharmacologically increased PP2A activity in these cancer cells barely ameliorates centromeric cohesion. These results suggest that compromised PP2A activity, a common phenomenon in cancer cells, may not be responsible for weak centromeric cohesion. Furthermore, centromeric cohesion in cancer cells can be strengthened by ectopic Sgo1 overexpression and weakened by SET WT, not by Sgo1-binding-deficient mutants. Altogether, these findings demonstrate that SET overexpression contributes to impaired centromeric cohesion in cancer cells and illustrate misregulated SET-Sgo1 pathway as an underlying mechanism.

## Monitoring Editor

Kerry Bloom  
University of North Carolina,  
Chapel Hill

Received: Dec 17, 2020

Revised: Apr 14, 2021

Accepted: Apr 20, 2021

## INTRODUCTION

Chromosome instability (CIN) leading to aneuploidy usually derives from chromosome missegregation during cell division. In cancer cells, several cellular defects that contribute to chromosome missegregation, including multiple spindle poles (Ganem *et al.*, 2009), weak centromeric cohesion (Barber *et al.*, 2008; Sajesh *et al.*, 2013; Stoecker *et al.*, 2015), and increased kinetochore-microtubule stability (Bakhom *et al.*, 2009), have been revealed. These mitotic defects that existed in cancer cells could be the major factors driving CIN during tumorigenesis (Lengauer *et al.*, 1998). However, the underlying causes for these defects in cancer cells are poorly under-

stood. Here we study the mechanisms underlying weak centromeric cohesion in cancer cells.

Sister-chromatid cohesion is established during S phase and thereafter maintained until mitosis. At early mitosis, most of cohesin is released from chromosome arms, whereas a small pool of cohesin at centromeres is protected until anaphase onset when this pool of centromeric cohesin is cleaved by Separase to allow chromosome segregation. Protection of centromeric cohesion is carried out by the well-conserved complex of Shugoshin1 (Sgo1) and phosphatase 2A (PP2A) (Kitajima *et al.*, 2004, 2006; Riedel *et al.*, 2006; Tang *et al.*, 2006). Depletion of Sgo1 in human cells resulted in massive centromeric cohesion defects and cell death, demonstrating the essential role of Sgo1 in centromeric cohesion protection (Tang *et al.*, 2004). As an essential cohesin protector, Sgo1 might be an ideal mutation target for weakening centromeric cohesion in the process of cancer development. However, mutations in Sgo1 have rarely been identified in cancer cells (Lawrence *et al.*, 2014), suggesting that instead of Sgo1 per se, other factors including Sgo1 regulators might selectively be mutated in tumorigenesis. Thus, it is very attractive to identify such factors and then determine how their misregulation contributes to weak centromeric cohesion in cancer cells.

To enable its function of cohesion protection, Sgo1 must be installed onto cohesin at the inner centromere (the place between two sister centromeres) at early mitosis (Tang *et al.*, 2004; Kawashima *et al.*, 2010, 2005). This process requires Bub1-dependent histone

This article was published online ahead of print in MBoC in Press (<http://www.molbiolcell.org/cgi/doi/10.1091/mbc.E20-12-0778>) on April 28, 2021.

The authors declare no competing financial interests.

Author contributions: conceptualization, H.L.; methodology, H.L.; investigation, L.Y., Q.Z., and H.L.; statistical analysis, L.Y., Q.Z., T.N., and H.L.; writing—original draft, H.L.; writing—review and editing, L.Y., Q.Z., T.N., and H.L.; funding acquisition, H.L.; resources, H.L.; supervision, H.L.

\*Address correspondence to: Hong Liu (hliu22@tulane.edu).

Abbreviations used: CIN, chromosome instability; FBS, fetal bovine serum; PBS, phosphate-buffered saline; PP2A, phosphatase 2A; Sgo1, Shugoshin1.

© 2021 Yang *et al.* This article is distributed by The American Society for Cell Biology under license from the author(s). Two months after publication it is available to the public under an Attribution–Noncommercial–Share Alike 3.0 Unported Creative Commons License (<http://creativecommons.org/licenses/by-nc-sa/3.0>).

“ASCB®,” “The American Society for Cell Biology®,” and “Molecular Biology of the Cell®” are registered trademarks of The American Society for Cell Biology.

H2A phosphorylation (Kawashima *et al.*, 2010), which promotes Sgo1 binding to nucleosomes (Liu *et al.*, 2015), and Cdk1-mediated Sgo1 phosphorylation, which promotes Sgo1 binding to cohesin (Liu *et al.*, 2013b; Hara *et al.*, 2014). At anaphase onset, Sgo1 must be removed away from centromeric cohesin to allow timely chromosome segregation (Liu *et al.*, 2013a). SET, a previously identified PP2A inhibitor (Li *et al.*, 1995; 1996), has recently been shown to remove Sgo1 from centromeres by directly binding Sgo1, thereby disabling Sgo1 functions at anaphase onset (Krishnan *et al.*, 2017; Qu *et al.*, 2019). Thus, an elaborate network during mitosis ensures accurate and appropriate regulation of Sgo1 in time and space. Misregulation of this network could compromise Sgo1 functions, thus weakening centromeric cohesion. Interestingly, extensive studies have demonstrated that high SET protein levels and decreased PP2A activity are common phenomena in cancer cells (Chen *et al.*, 2004; Neviani *et al.*, 2005; Hung and Chen, 2017), leading to a proposal that misregulated SET-PP2A pathway may contribute to tumorigenesis (Hung and Chen, 2017). Given the important roles of SET and PP2A in centromeric cohesion regulation, one would hypothesize that increased SET protein levels and decreased PP2A activity might be the major factors contributing to weak centromeric cohesion in cancer cells. Alternatively, as SET binds Sgo1 and serves as a Sgo1 inhibitor (Krishnan *et al.*, 2017; Qu *et al.*, 2019), it is possible that high-level SET protein could directly impair Sgo1 functions, resulting in attenuated centromeric cohesion (Zhang and Liu, 2020). However, these attractive hypotheses have never been tested. Here, we address these questions by examining centromeric cohesion in 26 cell lines from various types of cancers. We found that overexpressed SET protein in cancer cells contributes to weak centromeric cohesion. SET may achieve it through Sgo1.

## RESULTS

### SET protein overexpression is a common phenomenon in cancer cells

Various studies have demonstrated that SET protein is overexpressed in diverse types of cancer cells and tissues (Hung and Chen, 2017). To confirm this, we examined the SET protein levels in 26 cancer cell lines from various cancer types (Figure 1A and Supplemental Figure S1B). Several nontransformed cells, including RPE-1, AG09266, AG08433, and BJ-fibroblast cells, were used in this study as control cell lines. Log-phase cells were used to examine SET protein levels as they seemed not to significantly change between in interphase and in mitosis (Supplemental Figure S1A). The cancer and nontransformed cells were randomly selected based on availability. To compare SET protein levels among these cell lines, we first examined SET and actin proteins by Western blots and normalized the levels of SET (both isoforms together) to the ones of actin (relative SET protein levels) in each cell line. We found that the relative SET protein levels in the four nontransformed cells were the lowest among all the tested cell lines (Supplemental Figure S1, B and C) and almost all of the tested cancer cell lines exhibited higher SET protein levels than the control cells. As the levels of many proteins are elevated in cancer cells (Thiru *et al.*, 2014), using actin to normalize SET may not be accurate. We therefore renormalized the levels of the SET protein to the ones of total proteins, as revealed by GelCode Blue staining (Figure 1A). Overall, the relative SET protein levels in the majority of the tested cancer cells were still elevated compared with the control cells, but the elevated extents were less than the ones calculated based on the actin protein levels (Figure 1B), suggesting that actin is also overexpressed in most of the cancer cells. Hence, we decided to utilize the relative SET protein levels normalized to total protein levels for further analysis. Based on

these results, we conclude that SET is overexpressed in cancer cells, which is consistent with the previous findings (Hung and Chen, 2017).

### Cancer cells with high SET protein levels tend to exhibit weak centromeric cohesion

We then examined the robustness of centromeric cohesion in these cancer cells. MG132 rather than nocodazole was selected in this study because MG132 can induce cohesion fatigue, which can be used to detect mild cohesion defects (Daum *et al.*, 2011; Sapkota *et al.*, 2018; Qu *et al.*, 2019). By quantifying unseparated and separated sister chromatids (Figure 2A), we scored the robustness of centromeric cohesion. Overall, only a small portion of all the tested nontransformed cells exhibited the phenotype of separated sister chromatids in the presence of MG132 (Supplemental Figure S2B); in contrast, among the 26 tested cancer cell lines, 21 of them exhibited weaker centromeric cohesion than nontransformed RPE-1 cells (Figure 2A; Supplemental Figure S2, A and C), consistent with the previous observations that centromeric cohesion was impaired in cancer cells (Barber *et al.*, 2008; Sajesh *et al.*, 2013; Stoepker *et al.*, 2015). These results raised a possibility that high-level SET protein might be a major factor contributing to weak centromeric cohesion in cancer cells. Of note, DLD-1, MCF7, C4-2, and LNCaP cells were found to exhibit as robust centromeric cohesion as RPE-1 cells, although their SET protein levels were higher than the ones in RPE-1 cells (Figures 1B and 2A). The underlying mechanisms about the four outliers will be discussed later. To better understand the relationship between relative SET protein levels and centromeric cohesion robustness, we performed Pearson's correlation analysis among all 26 cancer cells and RPE-1 cells and found that they were moderately positively correlated ( $r = 0.3480$ ,  $p = 0.0753$ ), which reached a marginal statistical significance (Figure 2B) (Hu *et al.*, 2017; Schober *et al.*, 2018). Based on the above findings, we conclude that cancer cells with elevated SET protein levels tend to exhibit weak centromeric cohesion.

### Partial SET knockdown strengthens centromeric cohesion in cancer cells

We next sought to determine whether high levels of SET protein contribute to centromeric cohesion in cancer cells. A total of seven cancer cell lines that exhibited severer centromeric cohesion were selected: HeLa Tet-On, H460, SW480, Phoenix, Hep G2, HT-29, and COS-1. To test if overexpressed SET protein could promote weak centromeric cohesion in these cancer cells, we decided to partially knock down SET protein in cancer cells. Western blots verified that SET siRNAs decreased the SET protein levels (Figure 3A). Under such conditions, partial SET knockdown significantly rescued their centromeric cohesion defects in all the tested cancer cells treated with MG132 (Figure 3B). In addition, the rescue was also observed in HeLa Tet-On cells treated with another distinct SET siRNA oligo. Thus, overexpressed SET protein contributes to weak centromeric cohesion in cancer cells.

### Partial SET knockdown that strengthens centromeric cohesion does not increase overall PP2A activity in cancer cells

We then tried to determine the underlying mechanisms whereby high-level SET protein impairs centromeric cohesion in cancer cells. Given the previous findings that SET is a PP2A inhibitor and PP2A activity is essential for centromeric cohesion (Li *et al.*, 1995, 1996; Kitajima *et al.*, 2006; Riedel *et al.*, 2006; Tang *et al.*, 2006), we tested if increased PP2A activity could be responsible for the amelioration

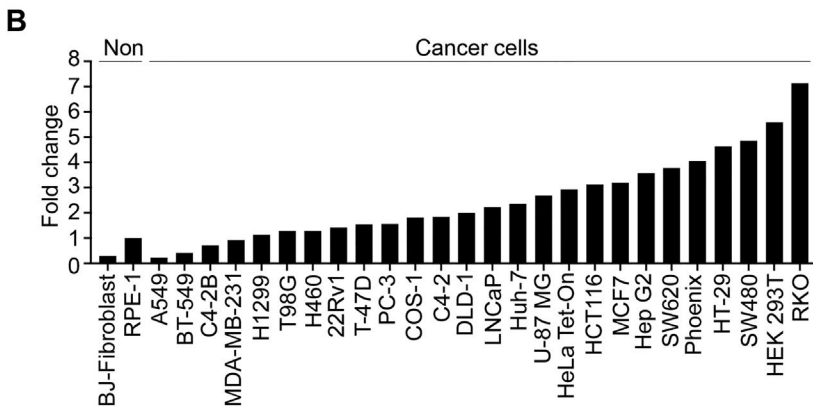
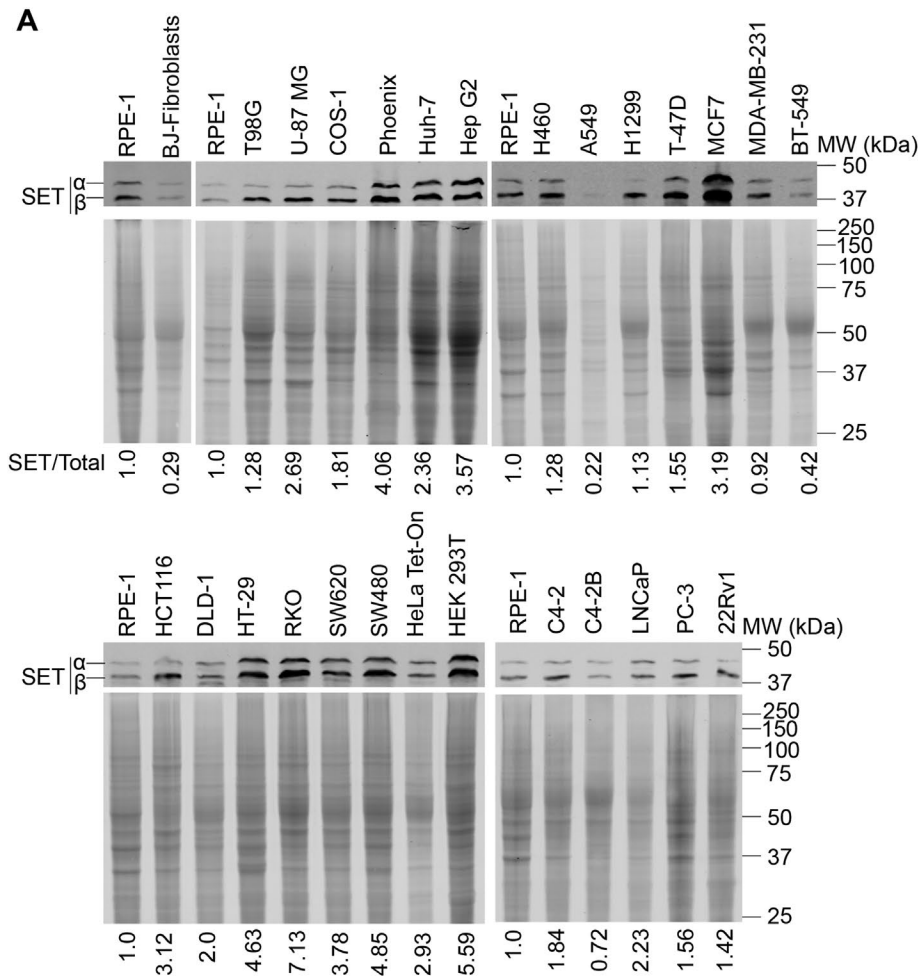


**FIGURE 1:** SET protein is overexpressed in various types of cancer cells. (A) Lysates from the indicated cell lines were resolved with SDS-PAGE, stained with Gelcode Blue, and blotted with anti-SET antibody. The relative SET protein level in each cancer cell line was obtained from the SET/actin ratio. The relative SET protein level in each cancer cell line was then normalized to the one in RPE-1 and fold change is shown in the bottom panels. The quantification details here and in the other figures were recorded in *Materials and Methods*. (B) Column view of quantification of SET protein levels in A. Non denotes nontransformed.

of centromeric cohesion in these cancer cells on SET knockdown. Akt phosphorylation at Ser473 was extensively used as an indicator to measure PP2A activity (Samanta *et al.*, 2009; Switzer *et al.*, 2011; Hu *et al.*, 2015). If SET knockdown-mediated enhancement of cen-

### Pharmacologically increased PP2A activity does not strengthen centromeric cohesion in cancer cells

We have shown that partial SET knockdown in cancer cells did not increase overall PP2A activity, but still significantly rescued

centromeric cohesion in cancer cells was caused by a general increase in PP2A activity, Akt Ser473 phosphorylation would be expected to decrease. As a comparison, partial SET knockdown used in Figure 3 was also applied here. Western blots showed that SET protein levels were decreased by SET siRNA treatment in all the tested cell lines (Figure 4A). Surprisingly, although Akt Ser473 phosphorylation was marginally decreased in COS-1 and Hep G2 cells, it was not decreased in the rest of the six cell lines; instead, it was increased in five cell lines including the nontransformed RPE-1 cells. As PP2A has many substrates, it is possible that distinct PP2A substrates may exhibit differential sensitivities to alteration in PP2A activity. Phosphorylations of Sororin and Hec1, both of which regulate kinetochore functions, have been suggested to be regulated by PP2A (Liu *et al.*, 2013b; Asai *et al.*, 2019), especially Sororin phosphorylation regulates sister-chromatid cohesion. We therefore examined their phosphorylations on partial SET knockdown. Surprisingly, immunostaining demonstrated that partial SET knockdown did not notably decrease; instead, it slightly increased the phospho-Hec1 (phospho Ser55) levels at kinetochores in MG132-arrested HeLa Tet-on and H460 cells. (Figure 4, B and C). The increase in phospho-Hec1 might be caused by SET knockdown-induced chromosome misalignment (Asai *et al.*, 2019). In addition, Western blots showed that partial SET knockdown only marginally decreased the phosphorylation levels of total Sororin (slow-migration WB bands, Figure 4D) and slightly increased phospho-Hec1 (phospho Ser55, Figure 4D) both in nocodazole-arrested HeLa Tet-On and H460 cells. Moreover, partial SET knockdown did not alter the phosphorylation of Sgo1-bound Sororin in nocodazole-arrested HeLa Tet-On cells (Supplemental Figure S3A). These results suggest that partial SET knockdown can improve centromeric cohesion without causing a detectable change in overall PP2A activity. Surprisingly, our results were inconsistent with a recent study reporting that SET depletion moderately decreased the levels of phospho-Hec1 (Asai *et al.*, 2019). The discrepancy could be due to the distinct experimental conditions of SET depletion. In our experiments, SET was only partially knocked down and its remaining levels were still comparable to the ones in RPE-1 cells.

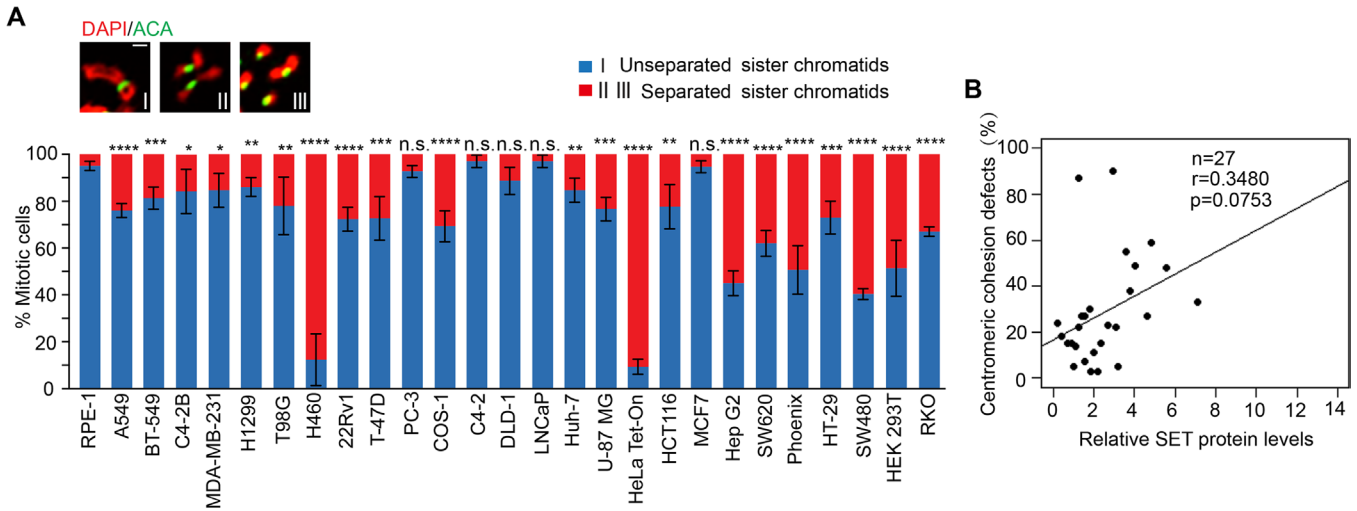


**FIGURE 2:** Cancer cells with high-level SET protein often exhibit weak centromeric cohesion. (A) RPE-1 and cancer cells were treated with MG132 for 6 h and the collected mitotic cells were subjected to chromosome spread and immunostaining with the indicated antibodies. In the top panel, representatives of spread chromosomes stained with DAPI and ACA are shown. Three categories of chromosome morphology were observed and are shown here: I, two sister centromeres cohesed; II, two sister centromeres separated but two sister chromatids still paired; III, sister centromeres completely scattered. The scale bar represents 1  $\mu$ m. In the bottom panel, quantification of separated (II and III) and unseparated d chromosomes (I) in cancer cells treated with MG132 for 6 h are shown. Mean and SD were calculated from at least three independent experiments. At least 20 mitotic cells were evaluated for each condition in every individual experiment. \* $P < 0.05$ ; \*\* $P < 0.01$ ; \*\*\* $P < 0.001$ ; \*\*\*\* $P < 0.0001$ ; n.s., no significance. (B) Pearson's correlation analysis on relative SET protein levels (Figure 1) and centromeric cohesion defects in A among all the 26 cancer cells and RPE1. Scatter plot with linear regression is shown here.

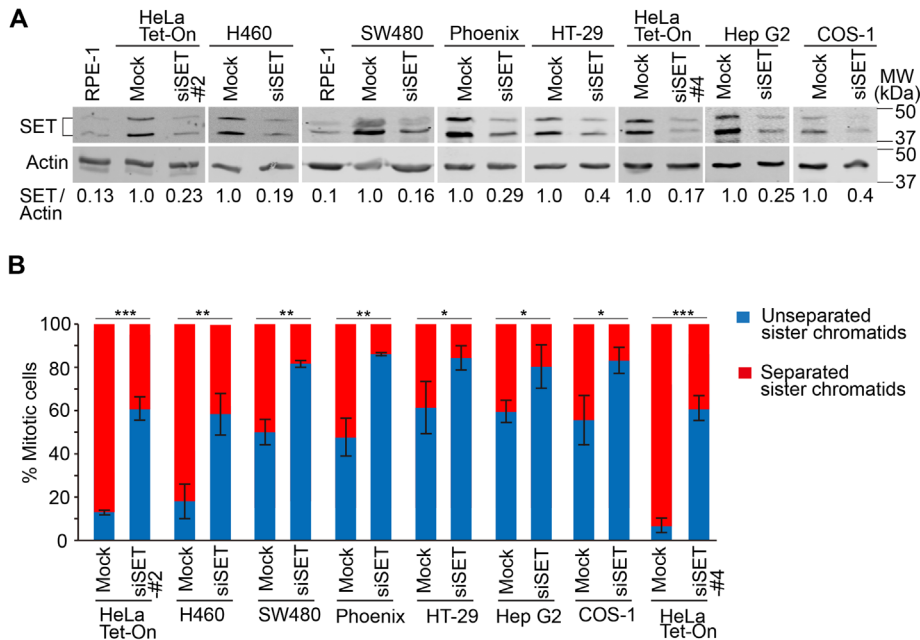


**FIGURE 3:** Partial SET knockdown largely increases centromeric cohesion in cancer cells. (A) Cells treated with mock or SET siRNA were incubated with MG132 for 4 h before harvest. Cell lysates were resolved with SDS-PAGE and blotted with the indicated antibodies. Two distinct siSET oligos (#2 and #4) were used to knock down SET protein in HeLa Tet-On cells. Other cell lines were treated with the oligo #4. The samples for each individual cancer cell were analyzed on different SDS-PAGE. The relative SET/actin ratio is shown in the bottom panel. (B) Partial SET knockdown largely suppresses centromeric cohesion defects in MG132-treated cancer cells. The cancer cells in A were subject to chromosome spread. Separated and unseparated sister chromatids were scored according to Figure 2A. Mean and SD were calculated based on at least three independent experiments. At least 25 mitotic cells were evaluated for each condition. \* $P < 0.05$ ; \*\* $P < 0.01$ ; \*\*\* $P < 0.001$ .

centromeric cohesion defects in the presence of MG132. We then wanted to know if pharmacologically increasing PP2A activity in these cancer cells could strengthen centromeric cohesion. To test it, we examined how the two chemicals, FTY720 and OP449 that were extensively used to enhance PP2A activity in cancer cells likely through disrupting the physical interaction between PP2A and SET (Arriazu *et al.*, 2016; Richard *et al.*, 2016; Szymiczek *et al.*, 2017; Fujiki *et al.*, 2018; O'Connor *et al.*, 2018), affected centromeric cohesion. Two cancer cell lines, HeLa Tet-On and H460, were selected because they exhibited the strongest centromeric cohesion defects (Figure 2A). As shown in Supplemental Figure S3B, FTY720 treatment largely decreased the Akt Ser473 phosphorylation levels in HeLa Tet-On cells in a time-dependent manner. OP449 treatment also significantly decreased them albeit less efficiently than FTY720. Although these two chemicals efficiently increased PP2A activity in cancer cells, neither of them significantly rescued centromeric cohesion defects in MG132-treated HeLa Tet-On cells (Supplemental Figure S3C). Similar results were also observed in MG132-treated H460 cells (Supplemental Figure S3, B and C). FTY20 was recently shown to release PP2A- $\alpha$  from SET by preventing SET dimerization or oligomerization, thus activating PP2A (De Palma *et al.*, 2019). We then

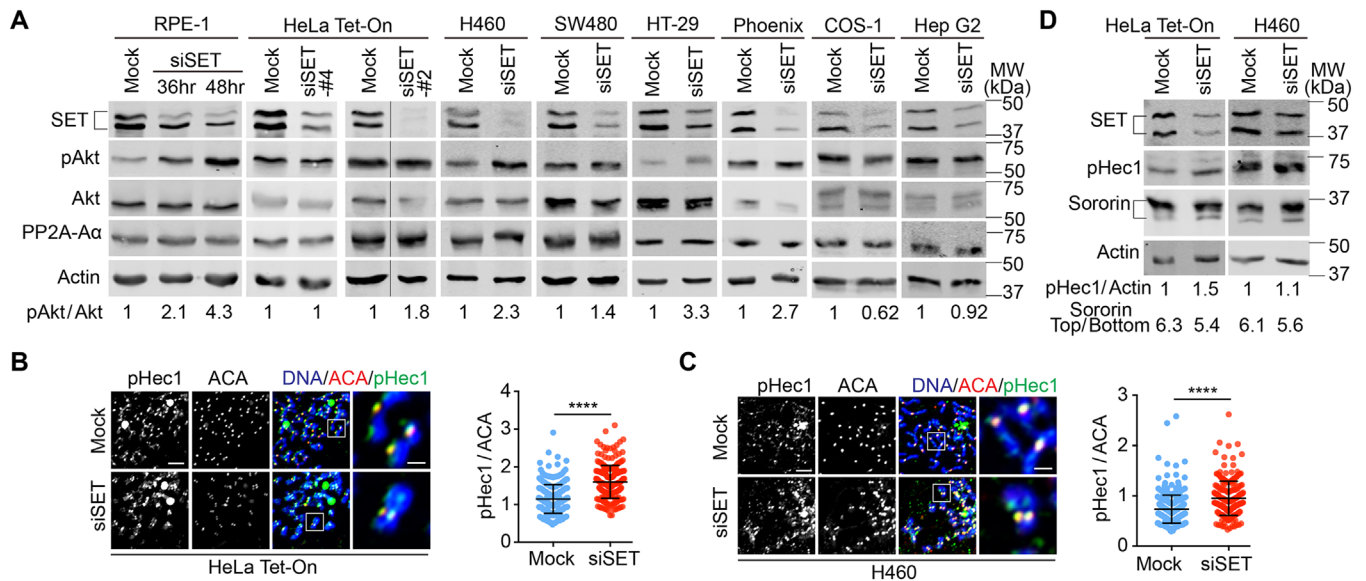


**FIGURE 4:** Partial SET knockdown does not cause overall change in PP2A activity. (A) Partial SET knockdown does not alter Akt phosphorylation (Ser473) in cancer cells. Lysates of the indicated cell lines with mock or SET siRNA treatment were resolved with SDS-PAGE and blotted with the indicated antibodies. Two distinct siSET oligos (#2 and #4) were used to knock down SET protein in HeLa Tet-On cells. Other cell lines were treated with the oligo #4. (B, C) Partial SET knockdown does not change Hec1 phosphorylation (phospho Ser55) in MG132-arrested HeLa Tet-On and H460 cells. Mock and siSET-treated HeLa Tet-On (B) and H460 (C) cells were incubated with MG132 for 2 h and mitotic cells were collected and subjected to immunostaining with the indicated antibodies. Representative images are shown in the left panels and quantifications of relative pHec1 levels (pHec1/ACA) are shown in the right panels. Quantification details were recorded in *Materials and Methods*. The mean and SD are shown here. At least 90 centromeres (6 per cell) were scored for each condition. The scale bars in the left and right panels represent 5 and 1 μm, respectively. (D) Partial SET knockdown does not decrease Hec1 phosphorylation (phospho Ser55) and Sororin phosphorylation (slow-migration WB bands) in nocodazole-arrested HeLa Tet-On and H460 cells. Mock and siSET-treated HeLa Tet-On and H460 cells were incubated with nocodazole for 2 h and cell lysates were subjected to Western blotting analysis with the indicated antibodies.

tested if FTY720 also affected the SET-Sgo1 interaction. Immunoprecipitation clearly showed that both FTY720 and OP449 did not notably alter the SET-Sgo1 interaction (Supplemental Figure S3D). Thus, compromised PP2A activity may not be a major cause for weak centromeric cohesion in cancer cells.

### Sgo1/SET ratios in cancer cells

As SET has been shown to be an inhibitor to Sgo1 (Krishnan *et al.*, 2017; Qu *et al.*, 2019), overexpressed SET protein in cancer cells might compromise Sgo1 functions, thus weakening centromeric cohesion. SET was also able to disrupt the Sgo1-cohesin interaction in a dose-dependent manner both *in vitro* and *in vivo* (Qu *et al.*, 2019). Therefore, the Sgo1/SET ratio, not the amount of Sgo1 *per se*, could be more important to determine the robustness of centromeric cohesion. We then examined the Sgo1 protein levels, and based on them, calculated Sgo1/SET ratios in these cancer cells (Supplemental Figure S4A). The Sgo1/SET ratio in RPE-1 cells was defined with 1.0 and the ones in all the cancer cells were normalized to it. Correlation analysis on all the cancer cells did not show an obvious correlation between the relative Sgo1/SET ratios and the centromeric cohesion defects ( $r = -0.2586$ ,  $p = 0.202$ ) (Supplemental Figure S4B), suggesting that Sgo1/SET ratios may not play an important role in centromeric cohesion in cancer cells.

In spite of no clear correlation between Sgo1/SET ratios and centromeric cohesion defects, a tendency was still observed that several cancer cell lines exhibiting extremely severe centromeric cohe-

sion defects under MG132 had relatively lower Sgo1/SET ratios. These cancer cells included SW480, SW620, HeLa Tet-On, and H460, with the Sgo1/SET ratios 0.61, 0.55, 0.46, and 0.41, respectively. As stated above, four outliers (DLD-1, MCF7, C4-2, and LN-CaP) were identified that expressed SET protein at the higher levels but did not exhibit centromeric cohesion defects induced by MG132 (Figure 2B). Their relative Sgo1/SET ratios were 0.87, 0.65, 0.91, and 1.26, respectively. The Sgo1/SET ratios in the outlier group were higher than the ones in the above group containing SW480, HeLa Tet-On, and H460, suggesting that elevated Sgo1 protein in the outlier cancer cells may offset the cohesion defects caused by overexpressed SET protein.

### Ectopically overexpressing Sgo1 significantly strengthens centromeric cohesion in cancer cells

As we previously showed that SET-binding Sgo1 suppresses Sgo1 functions, we sought to examine if ectopically overexpressing Sgo1 could strengthen centromeric cohesion in cancer cells. We first tested expression of plasmids containing GFP-Sgo1 WT or the SET-binding-deficient mutant  $\Delta$ SET (Qu *et al.*, 2019) by Western blots in the previously selected seven cancer cell lines that exhibited severe centromeric cohesion defects (Figure 3). Only HeLa Tet-On, COS-1, and Phoenix cells expressed the transgenic Sgo1 at the high level; the rest of the four cell lines (SW480, HepG2, H460, and HT-29) poorly did so. Included as well was one more cell line HEK 293T that exhibited strong cohesion defects and was able to express the transgenes

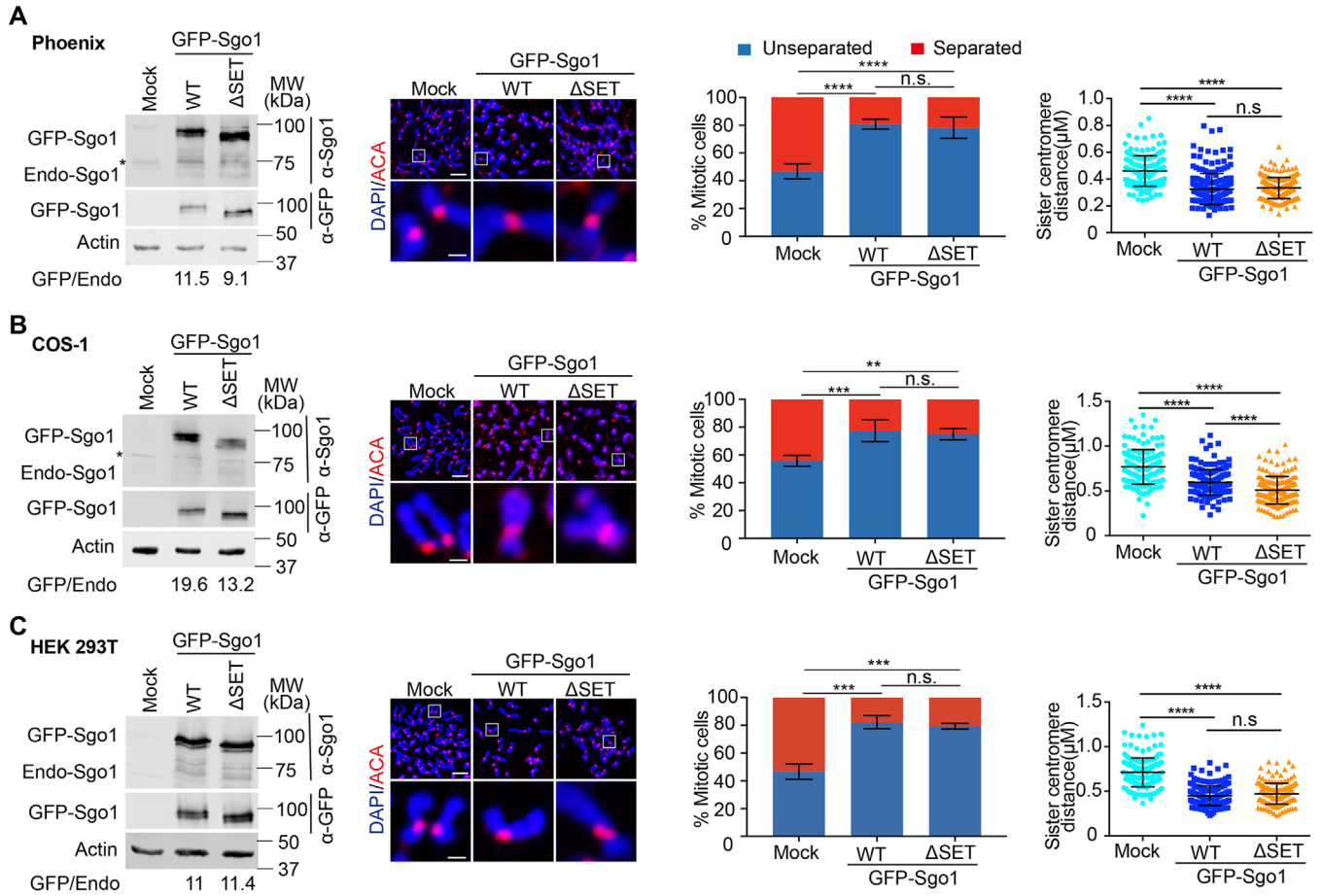


**FIGURE 5:** Ectopically overexpressing Sgo1 increases centromeric cohesion in cancer cells. Phoenix (A), COS-1 (B), and HEK 293T (C) cells transfected with plasmids containing GFP-Sgo1 WT or  $\Delta$ SET were treated with MG132 for 4 h before harvest. Then cells were subjected to chromosome spread followed by staining with the indicated antibodies. Cell lysate was also subjected to Western blot analysis with the indicated antibodies. Results of Western Blots are shown in the left panels and representative images are shown in the middle panels. Separated and unseparated sister chromatids were scored according to Figure 2A and recorded in the middle panels. Mean and SD were calculated from at least three independent experiments. At least 35 mitotic cells were evaluated for each condition. The sister-centromere distance was measured and recorded in the right panels. Mean and SD are shown here. At least 90 centromeres (6 per cell) were scored for each condition; n.s., no significance. \*\* $P < 0.001$ ; \*\*\* $P < 0.001$ ; \*\*\*\* $P < 0.0001$ . The scale bars in the top and bottom panels represent 5 and 1  $\mu\text{m}$ , respectively.

(Figure 5, A–C). Sgo1 overexpression was already shown to significantly suppress centromeric cohesion defects in MG132-treated HeLa Tet-On cells (Qu *et al.*, 2019). Similarly, ectopically overexpressing GFP-Sgo1 WT or  $\Delta$ SET in Phoenix, COS-1, and HEK 293T cells also significantly strengthened centromeric cohesion (Figure 5, A–C). GFP-Sgo1  $\Delta$ SET was expected to behave better in rescuing cohesion defects as it resisted SET inhibition (Qu *et al.*, 2019), but no significant difference between Sgo1 WT and delta-SET was observed in the tested cancer cells. The underlying reason might be that the expression levels of the two transgenes were too high (Qu *et al.*, 2019). Notably, about 40–50% of cancer cells overexpressing GFP-Sgo1 exhibited ectopic arm cohesion. At the same time, the sister-centromere distances were also significantly shortened in these cells with normal centromeric cohesion (Figure 5, A–C). Thus, both ectopic arm cohesion and enhanced centromeric cohesion contribute to the rescue in cohesion fatigue in cells overexpressing Sgo1. Based on these results, we conclude that Sgo1 overexpression can improve centromeric cohesion in cancer cells.

### Ectopically overexpressing SET WT, not the Sgo1-binding-deficient mutant, weakens centromeric cohesion in cancer cells

We have previously isolated two SET mutants (Qu *et al.*, 2019). Their functional analysis in cells would be key in mechanistically understanding how SET overexpression contributes to weak centromeric cohesion in cancer cells. Biochemical properties of SET WT and mutants were summarized in Figure 6A. SET WT binds both PP2A and Sgo1. The SET 3K mutant exhibits reduced Sgo1 binding but still retains the ability of PP2A binding; the other mutant SET  $\Delta$ C loses its binding to both PP2A and Sgo1. Thus, 3K is a mutant that may dissect the distinct functions of SET in regulating PP2A and Sgo1 in cells. Nontransformed RPE-1 cells stably expressing SET ( $\alpha$ ) WT, 3K, or  $\Delta$ C were constructed. Western blots showed that these transgenes were overexpressed compared with their endogenous counterparts (Figure 6B). Under such overexpression, both SET WT and 3K significantly suppressed PP2A activity, as revealed by increased Akt Ser473 phosphorylation, confirming that 3K is a separation-of-function mutant. Expectedly, SET  $\Delta$ C that

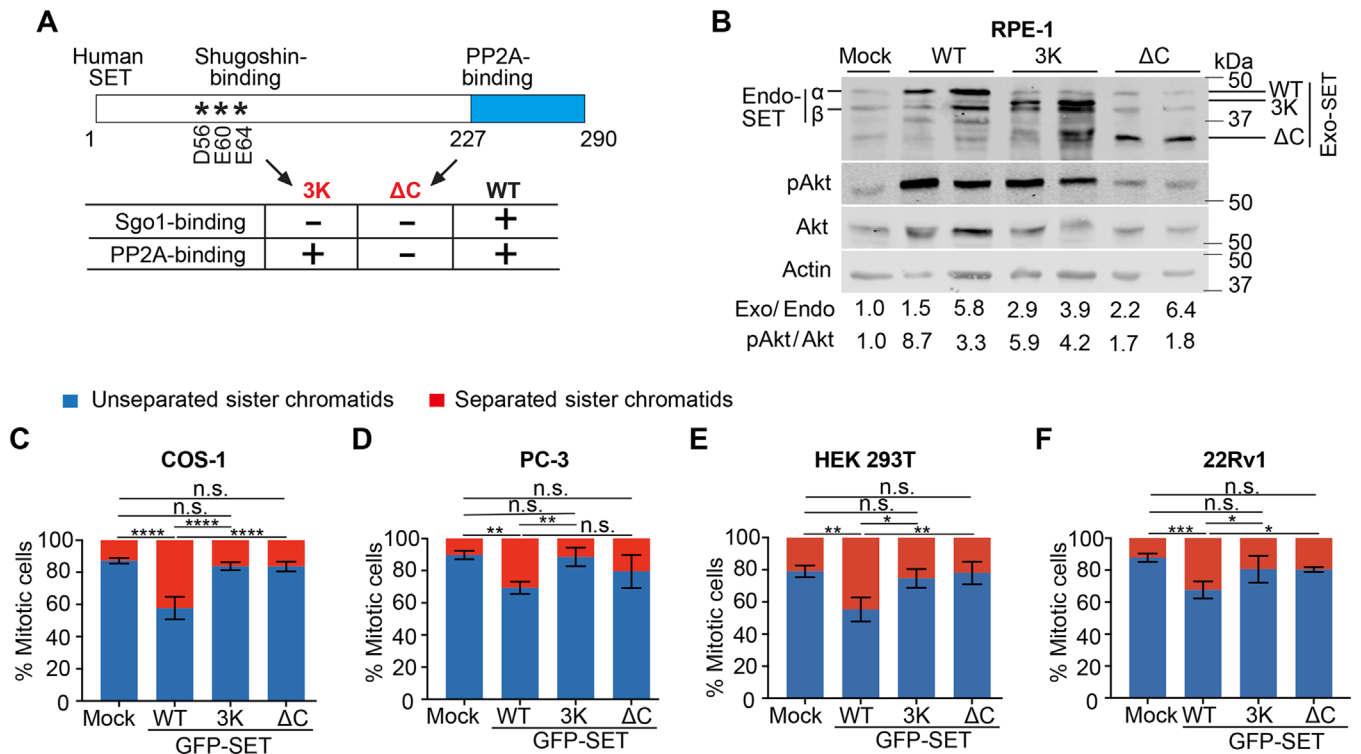


**FIGURE 6:** Overexpression of SET WT, not the Sgo1-binding-deficient mutant 3K, further weakens centromeric cohesion in cancer cells. (A) Summary of the biochemical properties of SET WT, 3K, and ΔC. It was based on our previous study (Qu *et al.*, 2019). (B) Lysates of RPE1 stably expressing SET (α) WT, 3K, or ΔC were resolved with SDS-PAGE and blotted with the indicated antibodies. C-F, COS-1 (C), PC-3 (D), HEK 293T (E), and 22Rv1 (F) cells transfected with plasmids containing GFP-SET WT, 3K, or ΔC were treated with MG132 for 2 h before harvest. Then cells were subjected to chromosome spread. Separated and unseparated sister chromatids were scored according to Figure 2A. Mean and SD calculated from at least three independent experiments are shown here. At least 20 mitotic cells were evaluated for each condition. n.s., no significance. \* $P < 0.05$ ; \*\* $P < 0.01$ ; \*\*\* $P < 0.001$ ; \*\*\*\* $P < 0.0001$ .

failed to bind PP2A almost lost its ability of PP2A inhibition. Furthermore, our previous results demonstrated that overexpression of SET WT, not 3K, significantly weakened centromeric cohesion in MG132-arrested RPE-1 cells (Qu *et al.*, 2019), functionally supporting the notion that SET overexpression induces centromeric cohesion defects through Sgo1.

To further validate the above notion, we also examined how overexpression of these SET transgenes affected centromeric cohesion in cancer cells. PC-3, 22Rv1, and COS-1 cells were selected because their endogenous SET protein levels were just slightly elevated compared with RPE-1 cells (Figure 1). HEK 293T cells, although they expressed SET protein at a much higher levels, were also included as they efficiently expressed the transgenes. The four cell lines were transfected with plasmids containing GFP-SET (α) WT, 3K, or ΔC, and centromeric cohesion was assessed after a 2-h MG132 treatment. Shorter MG132 treatment here was applied to ensure lower centromeric cohesion defects in mock-treated cells, thus enabling us to better dissect the effects of these SET transgenes. Western blots demonstrated that the SET transgenes were expressed at much higher levels than the endogenous counterparts (Supplemental Figure S5, A–D). Under such conditions, GFP-SET WT exacerbated centromeric cohesion defects in all the tested cancer cells, whereas 3K failed to do so (Figure 6, C–F), strongly suggesting that disruption of the Sgo1–cohesin interaction is responsible for the observed phenotype (Qu *et al.*, 2019). Moreover, GFP-SET ΔC also lost the ability to exacerbate centromeric

cohesion defects in the tested cancer cells. Surprisingly, overexpression of GFP-SET WT and 3K did not obviously decrease Akt Ser473 phosphorylation in the tested cancer cells, which is seemingly incongruent with the results obtained from RPE-1 cells (Figure 6B and Supplemental Figure S5, A–D). The underlying reasons are unknown and might be due to distinct genetic backgrounds between nontransformed and cancer cells. Nevertheless, even without notably altering overall PP2A activity, GFP-SET WT, not the Sgo1-binding deficient mutant 3K, still exacerbated centromeric cohesion defects in the tested cancer cells (Figure 6, C–F). Thus, SET overexpression can impair centromeric cohesion through Sgo1 in cancer cells.

## DISCUSSION

Consistent with the previous findings, we found that most cancer cells exhibit weak centromeric cohesion compared with nontransformed cells (Barber *et al.*, 2008; Sajesh *et al.*, 2013; Stoepker *et al.*, 2015). This universally existed defect in cancer cells could be a legacy inherited from tumorigenesis. Therefore, a better understanding of the molecular mechanisms underlying weak centromeric cohesion could help us decipher the driving forces for tumorigenesis. In this study, we have uncovered such a mechanism: universally overexpressed SET protein in cancer cells weakens centromeric cohesion.

How is centromeric cohesion attenuated in cancer cells? Although Sgo1 plays an essential role in centromeric cohesion

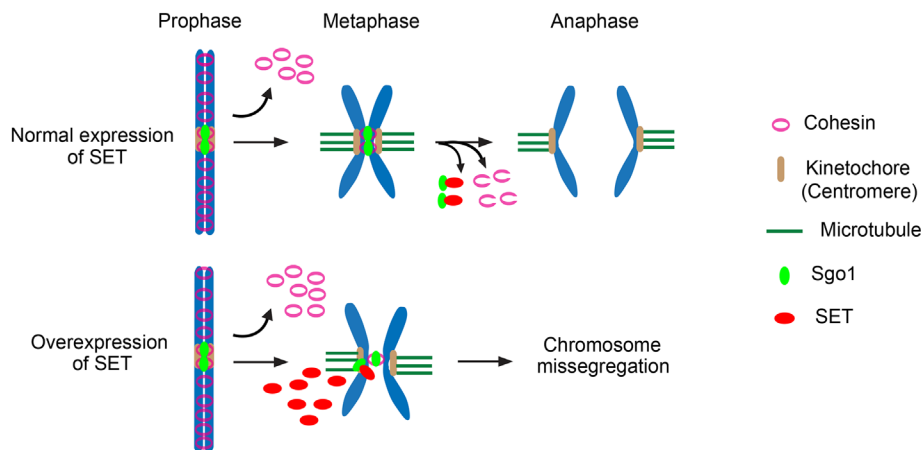


**FIGURE 7:** Working model. In normal cells, SET is expressed at low levels and it disables Sgo1 functions at metaphase to anaphase transition, thus promoting proper chromosome segregation. In cancer cells, SET is often overexpressed, which prematurely weakens centromeric cohesion, thus leading to chromosome missegregation.

protection, mutations in Sgo1 have rarely been identified in cancer cells (Lawrence *et al.*, 2014), suggesting that instead of Sgo1 *per se*, Sgo1 regulators might selectively be mutated or misregulated. In this study, we have identified such a factor, SET, originally characterized as a PP2A inhibitor. Several recent studies, including ours, demonstrated that SET is also a Shugoshin inhibitor (Krishnan *et al.*, 2017; Asai *et al.*, 2019; Qu *et al.*, 2019). Interestingly, SET has been found to be overexpressed in various types of cancer cells and tissues (Hung and Chen, 2017). All these findings potentiated SET as a saboteur to centromeric cohesion in cancer cells. This notion is further supported by the results from this study demonstrating that overexpressed SET protein is an important factor contributing to weak centromeric cohesion in cancer cells. Thus, in addition to affect cancer cell proliferation and growth through PP2A, overexpressed SET can also induce CIN, likely through Shugoshin. In the future, it would be tempting to test whether this is the case using animal models.

How does SET overexpression impair centromeric cohesion in cancer cells? Considering that SET is a PP2A inhibitor and PP2A plays an important role in centromeric cohesion protection (Li *et al.*, 1995, 1996; Kitajima *et al.*, 2006; Riedel *et al.*, 2006; Tang *et al.*, 2006), it is possible that this is achieved through direct inhibition of PP2A activity. However, our current findings suggest that SET overexpression-induced weak centromeric cohesion may not be through directly inhibiting PP2A activity. First, partial SET protein knockdown significantly ameliorated centromeric cohesion in cancer cells without significantly increasing overall PP2A activity, revealed by several PP2A substrates (Figure 4, A–D). Second, pharmacologically increased PP2A activity in cancer cells did not ameliorate centromeric cohesion (Supplemental Figure S3, B and C). Last, overexpression of the Sgo1-binding-deficient SET mutant (3K) failed to weaken centromeric cohesion, albeit it behaved similarly to SET WT in regulating PP2A activity (Qu *et al.*, 2019) (Figure 6). Thus, although compromised PP2A activity is a common phenomenon in cancer cells (Chen *et al.*, 2004; Neviani *et al.*, 2005), it may not directly contribute to weak centromeric cohesion. Instead, our findings reveal that overexpressed SET protein impairs centromeric cohesion, likely through directly attenuating Sgo1 functions in not all but at least some cancer cells. First, mutations of the three residues (3K mutant) in SET responsible for Sgo1 binding abrogated its capacity in weak-

ening centromeric cohesion when overexpressed (Qu *et al.*, 2019) (Figure 6). Interestingly, these mutations did not alter the ability of PP2A binding and inhibition (Figure 6). Second, overexpressing exogenous Sgo1 significantly ameliorated weak centromeric cohesion in cancer cells (Qu *et al.*, 2019) (Figure 5). Third, some cancer cell lines, such as LNCaP and C4-2, which had high-level SET protein but still exhibited as robust centromeric cohesion as RPE-1, simultaneously expressed Sgo1 protein at high levels (Supplemental Figure S4A). Thus, misregulated SET/Sgo1 pathway could be an important mechanism underlying weak centromeric cohesion in some cancer cells. Of course, it is possible that SET binding to Sgo1 enables its inhibition on Sgo1-bound PP2A activity. However, it is still directly through Sgo1 even though this possibility is true. A separation-of-function SET mutant that retains Sgo1 binding but abolishes PP2A inhibition would be necessary to conclusively address this point in future.

Of note, as the dynamic balance between spindle pulling forces and resistance to separation by interchromatid cohesion has been suggested to determine the rates of cohesion fatigue (Sapkota *et al.*, 2018), SET might also regulate cohesion fatigue through affecting this dynamic balance.

Consistent with our previous findings, a recent study demonstrated that SET can also bind Sgo2 (Asai *et al.*, 2019). They suggested that the Sgo2–SET interaction is important for the regulation of Aurora B activity and chromosome alignment at early mitosis but not for the protection of centromeric cohesion. Our previous results also suggested that SET is dispensable for centromeric cohesion protection at early mitosis; instead, it is important for centromeric cohesion deprotection at metaphase to anaphase transition (Qu *et al.*, 2019). Thus, SET may play various roles in regulating chromosome segregation at distinct cell cycle stages. At early mitosis, it binds Sgo2 to regulate chromosome alignment; at metaphase to anaphase transition, it binds Sgo1 to deprotect centromeric cohesion. In future, it would be interesting to explore how SET is regulated to tune Sgo2 and Sgo1 functions at distinct cell cycle stages.

In summary, based on all the available evidence, we propose that the misregulated Sgo1/SET pathway is an important mechanism underlying weak centromeric cohesion in cancer cells (Figure 7). In the future, it would be attractive to interrogate the roles of SET in tumorigenesis by expressing our isolated SET mutants in animal models.

## MATERIALS AND METHODS

### Mammalian cell culture, chemicals, siRNAs, and transfection

All the cell lines were cultured in the following media supplemented with 10% fetal bovine serum 10 mM L-glutamine and 10% Penicillin/Streptomycin: DMEM-F12, RPE-1; DMEM, HeLa Tet-On, COS-1, Phoenix, HEK 293T, T47-D, MCF7, BT-549, MDA-MB-231, H460, A549, H1299, Hep G2, Huh-7, C4-2B, HCT116, DLD-1, HT29, RKO, SW620, SW480, T98G, and U-87 MG, BJ-fibroblasts; RPMI1640, LNCaP, PC-3, 22Rv1, and C4-2. AG09266 and AG08433 were cultured with DMEM supplemented with 15% FBS and 1 mM L-glutamine. HeLa Tet-On and RPE-1 cells were authenticated through STR profiling by ATCC. All the other cell lines are gifts from the investigators listed in the *Acknowledgments*.

Nocodazole (M1404), MG132 (474790), and FTY720 (SML0700) were purchased from Sigma-Aldrich. OP449 was a gift from Oncotide Pharmaceuticals. The times for MG132, nocodazole, FTY720, and OP449 treatments were specified in each experiment.

To construct the stable cell lines, RPE-1 cells were infected with the lentiviral particles containing GFP-SET WT, 3K, or  $\Delta$ SET and selected with  $1\ \mu\text{g ml}^{-1}$  puromycin (Sigma).

To overexpress Sgo1 and SET, Sgo1 and SET (WT and mutants) cDNAs were inserted into PCS2-GFP vectors.

For RNAi experiments, the siRNA oligonucleotides were purchased from Thermo Scientific. Cells were transfected using Lipofectamine RNAiMax (Invitrogen) and analyzed at 36–48 h after transfection. The sequences of the siRNAs used in this study are: SET siRNA #2, GGAUGAAGGUGAAGAAGAU (Thermo Scientific, D-019586-02); SET siRNA #4, CGAGUCAACGCAGAAUAA (Thermo Scientific, D-019586-04).

### Construction of lentiviral particles

Lentiviral particles were generated using the pLVX-Puro system (Clontech) in HEK 293T cells. PEI:DNA complexes containing pRSV-Rev, pMDLg-pRRE, pMD2.G, and pLVX inserted of genes of interests (SET WT, 3K or  $\Delta$ C) were first prepared (Qu *et al.*, 2019). Then the assembled complexes were mixed into cultured HEK 293T cells. After 48 h, cell culture containing viruses was collected, filtered, and stored at  $-80^\circ\text{C}$  for later use.

### Antibodies and immunoblotting

The following antibodies were used in this study: anti-centromere antibody (ACA or CREST-ImmunoVision, HCT-0100), anti-PP2A- $\text{A}\alpha$  (Santa Cruz, Sc-6112), anti-Histone H3-pS10 (Cell signaling, 9706), anti-Smc1 (Bethyl, A300-055A), anti-SET (Bethyl, A302-261A), AKT (Cell signaling, 4691S), pAKT (S473) (Cell signaling, 4060S), anti-actin (Thermo Scientific, MA5-11869), anti-pHec1 (phospho Ser55, GTX70017, GeneTex), and anti-Myc (Millipore, 11667149001). Anti-Sororin is a gift from Susannah Rankin. Anti-Sgo1 and anti-GFP antibodies were made in-house as described previously (Liu *et al.*, 2013b; Kim and Yu, 2015).

Antibody dilution for immunoblotting was often 1:1000 unless specified.

The secondary antibodies were purchased from Li-COR: IRDye 680RD goat anti-mouse IgG secondary antibody (926-68070) and goat anti-rabbit IgG secondary antibody (926-32211).

Harvested cells were collected and lysed with SDS sample buffer. After being 5-min boiled, lysates were resolved by SDS-PAGE and blotted with indicated antibodies.

For immunoprecipitation, anti-myc or anti-GFP antibodies were coupled to Affi-Prep Protein A beads (Bio-Rad) at a concentration of  $1\ \text{mg ml}^{-1}$ .

### Immunoprecipitation

Immunoprecipitation in Supplemental Figure S3, A and D was performed as described before (Liu *et al.*, 2013b). HeLa Tet-On cells were dissolved in lysis buffer (25 mM Tris-HCl at pH 7.5, 50 mM NaCl, 5 mM  $\text{MgCl}_2$ , 0.1% NP-40, 1 mM DTT, 0.5  $\mu\text{M}$  okadaic acid, 5 mM NaF, and 0.3 mM  $\text{Na}_3\text{VO}_4$ ) containing 100  $\text{U ml}^{-1}$  Turbo-nuclease (Accelagen). After a 1-h incubation on ice followed by a 15-min incubation at room temperature, the lysate was cleared by centrifugation for 20 min at  $4^\circ\text{C}$  at  $20,817 \times g$ . The supernatant was then incubated with the beads precoupled with anti-Myc antibody (ThermoFisher, 20168) overnight at  $4^\circ\text{C}$ . After the beads were washed four times with wash buffer (25 mM Tris-HCl at pH 7.5, 100 mM NaCl, 5 mM  $\text{MgCl}_2$ , 0.1% NP-40, 1 mM DTT, 0.5  $\mu\text{M}$  okadaic acid,

5 mM NaF, and 0.3 mM  $\text{Na}_3\text{VO}_4$ ), the proteins bound to the beads were finally dissolved in SDS sample buffer, separated by SDS-PAGE, and blotted with the appropriate antibodies.

### Immunofluorescence and chromosome spread

For chromosome spreads and immunostaining in Figures 2A; 3B; 4, B and C; 5, A–C; 6, C–F; and Supplemental Figure S3C, collected MG132-treated mitotic cells were swelled in hypotonic solution containing 50 mM KCl for 15 min at room temperature and then spun onto slides with a Shandon Cytospin centrifuge. Cells were first extracted with ice-cold phosphate-buffered saline (PBS) containing 0.2% Triton X-100 for 2 min and then fixed in 4% ice-cold paraformaldehyde for 4 min. After being washed with PBS 0.1% Triton X-100, cells were sequentially incubated with primary antibodies (1:1000 dilution) overnight at  $4^\circ\text{C}$  and with the appropriate secondary antibodies conjugated to fluorophores (Invitrogen, A11008, A21090 and A31571, 1:1000 dilution) at room temperature for 1 h. Finally, cells were washed with PBS containing 0.1% Triton X-100, stained with  $1\ \mu\text{g ml}^{-1}$  DAPI, and mounted with Vectashield.

The images were taken by a Nikon confocal microscope with a 60 $\times$  objective. Image processing was carried out with ImageJ and Adobe Photoshop. Quantification was carried out with ImageJ.

### Quantification and statistical analysis

For quantification of SET protein levels in cells in Figure 1A, masks were generated to mark SET protein bands on WB membranes and each single lane on Gelcode Blue-stained SDS PAGE using the software of Image Studio Lite. After background subtraction, the intensities of SET proteins and total proteins within the masks were obtained in numeric values. The relative SET protein level in each cancer cell line was derived from the intensity of SET proteins normalized to the one of total proteins. Fold changes in the relative SET protein levels were compared between in RPE1 cells and in cancer cells and are shown in Figure 1, A and B.

For quantification of SET protein levels in cells in Supplemental Figure S1B, masks were generated to mark the desired protein bands on WB membranes using the software of Image Studio Lite. After background subtraction, the intensities of SET and actin protein bands within the masks were obtained in number. Relative SET protein levels in each cell were derived from the intensity of SET protein bands normalized to the one of actin protein bands. Fold changes in the relative SET protein levels were compared between in RPE1 cells and in cancer cells and are shown in Supplemental Figure S1, B and C.

For quantification of Sgo1/SET ratios in Supplemental Figure S4A, masks were generated to mark the desired protein bands on WB membranes using the software of Image Studio Lite. After background subtraction, the intensities of Sgo1 and SET protein bands within the masks were obtained in number. Sgo1/SET ratios in each cell were obtained from the normalization of the intensity of Sgo1 to the one of SET. Fold changes in Sgo1/SET ratios between RPE1 cells and in cancer cells and are shown in Supplemental Figure S4A.

Measurement of sister-centromere distance in Figure 5, A–C was performed using Image J. A straight line was drawn between a pair of sister centromeres, as indicated by ACA signals. Numeric values were automatically generated by ImageJ.

Pearson correlation analysis was applied in Figure 2B and Supplemental Figure 4SB. Pearson's correlation coefficient (Pearson's  $r$ ) and the  $p$  value (Schober *et al.*, 2018) were computed by using R software (R version 3.6.1, <https://www.r-project.org/>).

All experiments were repeated at least three times. Quantification was usually performed based on the results from all the repeated experiments unless specified. Differences were assessed using one-way ANOVA followed by pairwise comparisons using Tukey's test for the data in Figures 5, A–C and 6, C–F and Supplemental Figures S2B, S3C, and S5, A–D. In Figure 2A, differences between RPE-1 and each type of cancer cells were assessed using *T* tests. In Figures 3B and 4, B and C, differences between mock and siSET for each single cancer cell line were also assessed using *T* tests. All samples analyzed were included in quantification. Sample size was recorded in figures and their corresponding legends. No specific statistical methods were used to estimate sample size. No methods were used to determine whether the data meet assumptions of the statistical approach.

## ACKNOWLEDGMENTS

The Lentivirus system was a gift from Yan Dong at Tulane University Health Sciences Center. We also thank Brian G. Rowan, Hua Lu, Srikanta Dash, Zongbing You, Yan Dong, Zachary Pursell, David H Coy, Zhuo Wei, Hongtao Yu, and Sean Bong Lee for cell lines. OP449 is a gift from Oncotide Pharmaceuticals. This work was supported by the Tulane startup funds and National Institutes of Health P20GM103629 and R01GM124018 awarded to H.L.

## REFERENCES

Arriazu E, Pippa R, Odero MD (2016). Protein phosphatase 2A as a therapeutic target in acute myeloid leukemia. *Front Oncol* 6, 78.

Asai Y, Fukuchi K, Tanno Y, Koitabashi-Kiyozuka S, Kiyozuka T, Noda Y, Matsumura R, Koizumi T, Watanabe A, Nagata K, et al. (2019). Aurora B kinase activity is regulated by SET/TAF1 on Sgo2 at the inner centromere. *J Cell Biol* 218, 3223–3236.

Bakhoun SF, Genovese G, Compton DA (2009). Deviant kinetochore microtubule dynamics underlie chromosomal instability. *Curr Biol* 19, 1937–1942.

Barber TD, McManus K, Yuen KW, Reis M, Parmigiani G, Shen D, Barrett I, Nouhi Y, Spencer F, Markowitz S, et al. (2008). Chromatid cohesion defects may underlie chromosome instability in human colorectal cancers. *Proc Natl Acad Sci USA* 105, 3443–3448.

Chen W, Possemato R, Campbell KT, Plattner CA, Pallas DC, Hahn WC (2004). Identification of specific PP2A complexes involved in human cell transformation. *Cancer Cell* 5, 127–136.

Daum JR, Potapova TA, Sivakumar S, Daniel JJ, Flynn JN, Rankin S, Gorbysky GJ (2011). Cohesion fatigue induces chromatid separation in cells delayed at metaphase. *Curr Biol* 21, 1018–1024.

De Palma RM, Parnham SR, Li Y, Oaks JJ, Peterson YK, Szulc ZM, Roth BM, Xing Y, Ogretmen B (2019). The NMR-based characterization of the FTY720-SET complex reveals an alternative mechanism for the attenuation of the inhibitory SET-PP2A interaction. *FASEB J* 33, 7647–7666.

Fujiki H, Sueoka E, Watanabe T, Suganuma M (2018). The concept of the okadaic acid class of tumor promoters is revived in endogenous protein inhibitors of protein phosphatase 2A, SET and CIP2A, in human cancers. *J Cancer Res Clin Oncol* 144, 2339–2349.

Ganem NJ, Godinho SA, Pellman D (2009). A mechanism linking extra centrosomes to chromosomal instability. *Nature* 460, 278–282.

Hara K, Zheng G, Qu Q, Liu H, Ouyang Z, Chen Z, Tomchick DR, Yu H (2014). Structure of cohesin subcomplex pinpoints direct shugoshin-Wapl antagonism in centromeric cohesion. *Nat Struct Mol Biol* 21, 864–870.

Hu H, Zheng Y, Wang X, Chen B, Dong Y, Zhang J, Liu X, Gong D (2017). Correlations between lumbar neuromuscular function and pain, lumbar disability in patients with nonspecific low back pain: A cross-sectional study. *Medicine (Baltimore)* 96, e7991.

Hu X, Garcia C, Fazli L, Gleave M, Vitek MP, Jansen M, Christensen D, Mulholland DJ (2015). Inhibition of Pten deficient Castration Resistant Prostate Cancer by Targeting of the SET - PP2A Signaling axis. *Sci Rep* 5, 15182.

Hung MH, Chen KF (2017). Reprogramming the oncogenic response: SET protein as a potential therapeutic target in cancer. *Expert Opin Ther Targets* 21, 685–694.

Kawashima SA, Yamagishi Y, Honda T, Ishiguro K, Watanabe Y (2010). Phosphorylation of H2A by Bub1 prevents chromosomal instability through localizing shugoshin. *Science* 327, 172–177.

Kim S, Yu H (2015). Multiple assembly mechanisms anchor the KMN spindle checkpoint platform at human mitotic kinetochores. *J Cell Biol* 208, 181–196.

Kitajima TS, Hauf S, Ohsugi M, Yamamoto T, Watanabe Y (2005). Human Bub1 defines the persistent cohesion site along the mitotic chromosome by affecting Shugoshin localization. *Curr Biol* 15, 353–359.

Kitajima TS, Kawashima SA, Watanabe Y (2004). The conserved kinetochore protein shugoshin protects centromeric cohesion during meiosis. *Nature* 427, 510–517.

Kitajima TS, Sakuno T, Ishiguro K, Iemura S, Natsume T, Kawashima SA, Watanabe Y (2006). Shugoshin collaborates with protein phosphatase 2A to protect cohesin. *Nature* 441, 46–52.

Krishnan S, Smits AH, Vermeulen M, Reinberg D (2017). Phospho-H1 Decorates the Inter-chromatid Axis and Is Evicted along with Shugoshin by SET during Mitosis. *Mol Cell* 67, 579–593.e576.

Lawrence MS, Stojanov P, Mermel CH, Robinson JT, Garraway LA, Golub TR, Meyerson M, Gabriel SB, Lander ES, Getz G (2014). Discovery and saturation analysis of cancer genes across 21 tumour types. *Nature* 505, 495–501.

Lengauer C, Kinzler KW, Vogelstein B (1998). Genetic instabilities in human cancers. *Nature* 396, 643–649.

Li M, Guo H, Damuni Z (1995). Purification and characterization of two potent heat-stable protein inhibitors of protein phosphatase 2A from bovine kidney. *Biochemistry* 34, 1988–1996.

Li M, Makkinje A, Damuni Z (1996). The myeloid leukemia-associated protein SET is a potent inhibitor of protein phosphatase 2A. *J Biol Chem* 271, 11059–11062.

Liu H, Jia L, Yu H (2013a). Phospho-H2A and cohesin specify distinct tension-regulated Sgo1 pools at kinetochores and inner centromeres. *Curr Biol* 23, 1927–1933.

Liu H, Qu Q, Warrington R, Rice A, Cheng N, Yu H (2015). Mitotic Transcription Installs Sgo1 at Centromeres to Coordinate Chromosome Segregation. *Mol Cell* 59, 426–436.

Liu H, Rankin S, Yu H (2013b). Phosphorylation-enabled binding of SGO1-PP2A to cohesin protects sororin and centromeric cohesion during mitosis. *Nat Cell Biol* 15, 40–49.

Neviani P, Santhanam R, Trotta R, Notari M, Blaser BW, Liu S, Mao H, Chang JS, Galletta A, Uttam A, et al. (2005). The tumor suppressor PP2A is functionally inactivated in blast crisis CML through the inhibitory activity of the BCR/ABL-regulated SET protein. *Cancer Cell* 8, 355–368.

O'Connor CM, Perl A, Leonard D, Sangodkar J, Narla G (2018). Therapeutic targeting of PP2A. *Int J Biochem Cell Biol* 96, 182–193.

Qu Q, Zhang Q, Yang L, Chen Y, Liu H (2019). SET binding to Sgo1 inhibits Sgo1-cohesin interactions and promotes chromosome segregation. *J Cell Biol* 218, 2514–2528.

Richard NP, Pippa R, Cleary MM, Puri A, Tibbitts D, Mahmood S, Christensen DJ, Jeng S, McWeeny S, Look AT, et al. (2016). Combined targeting of SET and tyrosine kinases provides an effective therapeutic approach in human T-cell acute lymphoblastic leukemia. *Oncotarget* 7, 84214–84227.

Riedel CG, Katis VL, Katou Y, Mori S, Itoh T, Helmhart W, Galova M, Petronczki M, Gregan J, Cetin B, et al. (2006). Protein phosphatase 2A protects centromeric sister chromatid cohesion during meiosis I. *Nature* 441, 53–61.

Sajesh BV, Lichtensztejn Z, McManus KJ (2013). Sister chromatid cohesion defects are associated with chromosome instability in Hodgkin lymphoma cells. *BMC Cancer* 13, 391.

Samanta AK, Chakraborty SN, Wang Y, Kantarjian H, Sun X, Hood J, Perrotti D, Arlinghaus RB (2009). Jak2 inhibition deactivates Lyn kinase through the SET-PP2A-SHP1 pathway, causing apoptosis in drug-resistant cells from chronic myelogenous leukemia patients. *Oncogene* 28, 1669–1681.

Sapkota H, Wasiake E, Daum JR, Gorbysky GJ (2018). Multiple determinants and consequences of cohesion fatigue in mammalian cells. *Mol Biol Cell* 29, 1811–1824.

Schober P, Boer C, Schwarte LA (2018). Correlation coefficients: appropriate use and interpretation. *Anesth Analg* 126, 1763–1768.

Stoepker C, Ameziane N, van der Lelij P, Kooi IE, Oostra AB, Rooimans MA, van Mil SE, Brink A, Dietrich R, Balk JA, et al. (2015). Defects in the Fanconi anemia pathway and chromatid cohesion in head and neck cancer. *Cancer Res* 75, 3543–3553.

- Switzer CH, Cheng RY, Vitek TM, Christensen DJ, Wink DA, Vitek MP (2011). Targeting SET/1(2)PP2A oncoprotein functions as a multi-pathway strategy for cancer therapy. *Oncogene* 30, 2504–2513.
- Szymiczek A, Pastorino S, Larson D, Tanji M, Pellegrini L, Xue J, Li S, Giorgi C, Pinton P, Takinishi Y, et al. (2017). FTY720 inhibits mesothelioma growth in vitro and in a syngeneic mouse model. *J Transl Med* 15, 58.
- Tang Z, Shu H, Qi W, Mahmood NA, Mumby MC, Yu H (2006). PP2A is required for centromeric localization of Sgo1 and proper chromosome segregation. *Dev Cell* 10, 575–585.
- Tang Z, Sun Y, Harley SE, Zou H, Yu H (2004). Human Bub1 protects centromeric sister-chromatid cohesion through Shugoshin during mitosis. *Proc Natl Acad Sci USA* 101, 18012–18017.
- Thiru P, Kern DM, McKinley KL, Monda JK, Rago F, Su KC, Tsinman T, Yarar D, Bell GW, Cheeseman IM (2014). Kinetochore genes are coordinately up-regulated in human tumors as part of a FoxM1-related cell division program. *Mol Biol Cell* 25, 1983–1994.
- Zhang Q, Liu H (2020). Functioning mechanisms of Shugoshin-1 in centromeric cohesion during mitosis. *Essays Biochem* 64, 289–297.